Co-published by
Institute of Fluid-Flow Machinery
Polish Academy of Sciences
Committee on Thermodynamics and Combustion
Polish Academy of Sciences

http://www.imp.gda.pl/archives-of-thermodynamics/

Thermal Performance of MHD Radiative Nanofluid Convection over an Exponentially Stretching Surface in a Porous Medium

Adetayo Samuel Eegunjobi[a*], Oluwole Daniel Makinde[b]

[a]Mathematics Department, Namibia University of Science and Technology, Windhoek, Namibia
[b]Faculty of Military Science, Stellenbosch University, Private Bag X2, Saldanha 7395, South Africa
*Corresponding author email: samdet1@yahoo.com

Received: 21.02.2025; revised: 10.07.2025; accepted: 11.07.2025

Abstract

This study investigates the hydromagnetic convection of a radiating nanofluid flowing over an exponentially stretched sheet embedded in a porous medium, with emphasis on the influences of thermal radiation, magnetic fields, Joule heating, viscous dissipation, porous permeability, and nanoparticle volume fraction on flow and heat transfer behaviour. The governing momentum and energy equations are formulated using boundary layer theory and reduced to nonlinear ordinary differential equations via similarity transformations. We numerically solve these equations using the shooting method in conjunction with the Runge-Kutta-Fehlberg integration scheme. The analysis looks at how important factors like the strength of the magnetic field, thermal radiation, Prandtl number, and how easily fluid can flow through a porous material impact the system, showing how magnetic and thermal effects play a big role in how fluids move. One of the main discoveries is that stronger magnetic fields and more thermal radiation together lower the Nusselt number, highlighting the balance between heat transfer through radiation and convection, which is important in high-temperature industrial processes. The study offers important insights for optimising a range of engineering applications, including nanomaterial-based thermal coatings, energy systems, and magnetically influenced flow control that ultimately aid advancements in energy efficiency, manufacturing processes, and environmental technologies.

Keywords: Nanofluid; Magnetic field; Thermal radiation; Porous medium; Heat transfer

Vol. 46(2025), No. 4, 31–39; doi: 10.24425/ather.2025.156596

Cite this manuscript as: Eegunjobi, A.S., & Makinde, O.D. (2025). Thermal Performance of MHD Radiative Nanofluid Convection over an Exponentially Stretching Surface in a Porous Medium. *Archives of Thermodynamics*, 46(4), 31−39.

1. Introduction

Research on the hydromagnetic convection of radiative nanofluids over exponentially stretching sheets within porous media is highly significant, as it effectively tackles complex multiphysics problems encountered in engineering and applied sciences. Nanofluids, known for their superior thermal conductivity, play a vital role in enhancing heat transfer performance. Their response to the combined effects of magnetic fields, thermal radiation, and porous environments helps optimise diverse industrial processes [1]. Incorporating a porous medium enables realistic simulation of systems such as geothermal reservoirs, packed bed reactors and filtration units, while the exponentially stretching sheet models practical scenarios in manufacturing, including polymer extrusion, thin-film fabrication, and nanomaterial coating technologies [2]. The research also provides clarity regarding how magnetic fields affect fluid dynamics and energy transport, which is essential for applications such as electromagnetic pumps, magnetic damping systems, and magnetically actuated microfluidic devices. Additionally, the results can be used in high-efficiency thermal energy systems like solar collectors, heat exchangers, and thermal storage units, as well as in medical

Nomenclature

C_f – skin friction coefficient
C_p – specific heat capacity, J/(kg·K)
Da – Darcy number
Ec – Eckert number
k – thermal conductivity, $W \cdot m^{-1} \cdot K^{-1}$
k^* – mean absorption coefficient, m^{-1}
K – porous medium permeability, m^2
L – length, m
M – magnetic field parameter
Nu – Nusselt number
Pr – Prandtl number
q_r – radiative heat flux, $W \cdot m^{-2}$
q_w – local heat flux, $W \cdot m^{-2} \cdot$
Ra – thermal radiation parameter
Re_x – local Reynolds number
T, T_w, T_∞ – temperatures, K
u, v – velocity components (in the x, y directions, respectively), m/s
$U_w(x)$ – sheet exponential stretching velocity, m/s
x, y – directions, m

Greek symbols

μ – dynamic viscosity, Pa·s
ρ – density, kg/m^3
σ – electrical conductivity, $S \cdot m^{-1}$
σ^* – Stefan-Boltzmann constant, $W \cdot m^{-2} \cdot K^{-4}$
τ – wall shear stress, $N \cdot m^{-2}$
ϕ – volume fraction

Subscripts and Superscripts

f – fluid
nf – nanofluid
s – nanoparticles
w – sheet surface
∞ – free stream

Abbreviations and Acronyms

LTE – local thermal equilibrium
MHD– magnetohydrodynamic
ODE – ordinary differential equations

technologies such as targeted drug delivery using magnetic nanofluids and hyperthermia treatment. Additionally, the research contributes to advancements in geothermal and environmental engineering, supports efficient geothermal energy extraction, manages pollutant transport in aquifers, and prompts the development of magnetohydrodynamics (MHD) systems, including MHD generators and nuclear reactor cooling technologies.

The investigation of fluid flow over stretching surfaces has garnered significant attention due to its industrial relevance. Seminal work [3] on flow past a stretching plate laid the groundwork for further developments in this domain. Building on this, researchers such as those in [4–6] explored heat transfer over stretching surfaces under various boundary conditions, including scenarios involving variable surface heat flux. The influence of fluid properties like variable viscosity on flow and thermal behaviour was analysed in [7], highlighting the complexity of real-world applications. The incorporation of exponentially stretching surfaces introduced new dimensions to this field, allowing for the analysis of more intricate flow behaviours. As emphasised in [1], the unique geometry of exponentially stretching sheets, where the stretching rate increases exponentially with distance, has a profound effect on the fluid dynamics. Further studies [8–9] examined how surface curvature interacts with exponential stretching, offering valuable insights for optimising surface configurations in engineering systems. Research has also extended to different fluid types, with analysing second-grade fluids over stretching sheets [10] and investigating flow and heat transfer over curved surfaces [11], enriching the understanding of these complex flow environments.

The emergence of nanofluids has significantly transformed the landscape of heat transfer research. Notably, studies like [12] have investigated nanofluid flow over exponentially stretching sheets, taking into account critical factors such as thermal radiation, magnetic fields, and internal heat generation. These studies highlighted the capacity of nanofluids to enhance heat transfer performance in systems involving such stretching surfaces. The presence of nanoparticles dispersed in base fluids, which enhances properties like thermal conductivity, viscosity, and overall stability, is largely responsible for this improvement. A broad spectrum of research [13–16] has been dedicated to examining nanofluid dynamics under varied flow conditions. In particular, investigations in [17–20] have focused on flow and heat transfer over stretching surfaces while incorporating the influences of magnetic fields, heat sources, and radiation. Additionally, the influence of magnetic fields on nanofluid behaviour has been studied in detail [21–23], with findings emphasising the interaction between magnetic forces and fluid motion. Further studies have explored the impact of parameters such as Brownian motion, thermophoresis, heat generation or absorption, and the presence of porous media, offering valuable insights into optimising nanofluid-based heat transfer systems across a range of engineering applications.

Magnetohydrodynamics (MHD), which examines the interaction between electrically conducting fluids and magnetic fields, plays a pivotal role in various fields such as materials processing, astrophysics, and geophysics. Its principles underpin several advanced technologies, including MHD propulsion systems, power generation units, and electromagnetic pumps. Extensive research on MHD heat transfer in nanofluids has shed light on its unique thermal characteristics and flow behaviour. Studies [24–26] have specifically explored the influence of magnetic fields on flow dynamics, thermal radiation, and heat transfer, enhancing our comprehension of nanofluid performance under magnetic effects. Further investigations [27–29] into MHD nanofluid flow over stretching surfaces have examined how magnetic forces affect velocity fields, temperature profiles, and heat transfer rates. These works collectively highlight the intricate interplay between magnetic fields and buoyancy-driven convection, offering more profound insights into the complex thermal-fluid behaviour of nanofluids exposed to simultaneous magnetic and thermal influences. Several notable studies on hydromagnetic nanofluid convection over a stretching sheet can be found in Refs. [35–38].

In this study, we look at how several important factors, including magnetic field strength, the ability of the porous material to conduct magnetic fields, thermal radiation, heat loss due to fluid movement, the amount of nanoparticles, and Joule heating, affect the movement of a nanofluid flowing over a heated surface that stretches exponentially, especially regarding heat transfer. To the best of our knowledge, this kind of comprehensive analysis is scarcely addressed in the existing literature, aiming here to bridge that gap. The multifaceted approach provides helpful suggestions for enhancing heat transfer performance in complex systems where multiple physical effects interact simultaneously. Such investigations are essential for advancing thermal management strategies in critical applications, including electronic device cooling, metal extrusion, polymer manufacturing, nuclear reactor safety, and energy harvesting systems. By understanding how these parameters affect temperature profiles, flow dynamics, and heat transfer rates, engineers can develop more efficient, robust, and high-performance systems capable of functioning under extreme thermal and electromagnetic conditions. The subsequent sections detail the mathematical modelling, analytical framework, and numerical findings, accompanied by a thorough quantitative discussion.

2. Model description

We examine the laminar flow of a steady, two-dimensional, incompressible, viscous, electrically conducting, and radiative nanofluid over an exponentially stretching sheet embedded in a porous medium. The coordinate system is defined such that the x-axis lies along the surface of the sheet, while the y-axis is oriented normal to it. A transverse magnetic field of constant strength B_0 is applied perpendicular to the flow direction, as depicted in Fig. 1.

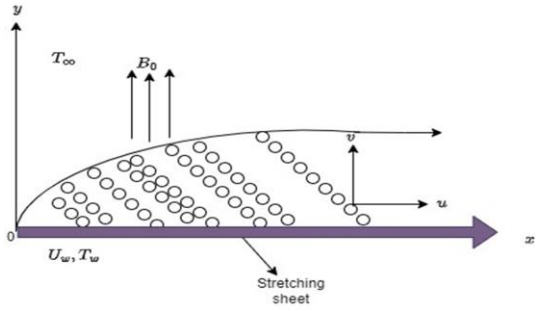

Fig. 1. Flow model diagram.

The induced magnetic field is considered negligible due to a low magnetic Reynolds number, and the Hall effect is disregarded, assuming a minimal overall current density. The porous medium, characterised by negligible inertia effects, and the nanofluid are assumed to be in local thermal equilibrium (LTE). Applying the standard boundary layer approximations, the governing continuity, momentum, and energy balance equations for the problem are formulated as follows [2,9,36,37]:

$$\frac{\partial u}{\partial x}+\frac{\partial u}{\partial y}=0, \tag{1}$$

$$u\frac{\partial u}{\partial x}+v\frac{\partial u}{\partial y}=\frac{\mu_{nf}}{\rho_{nf}}\frac{\partial^2 u}{\partial y^2}-\frac{\sigma_{nf}B_0^2 u}{\rho_{nf}}-\frac{\mu_{nf}u}{\rho_{nf}K}, \tag{2}$$

$$u\frac{\partial T}{\partial x}+v\frac{\partial T}{\partial y}=\frac{k_{nf}}{(\rho C_p)_{nf}}\frac{\partial^2 T}{\partial y^2}+\frac{\mu_{nf}}{(\rho C_p)_{nf}}\left(\frac{\partial u}{\partial y}\right)^2+\frac{\sigma_{nf}B_0^2u^2}{(\rho C_p)_{nf}}+$$
$$+\frac{\mu_{nf}u^2}{(\rho C_p)_{nf}K}-\frac{1}{(\rho C_p)_{nf}}\frac{\partial q_r}{\partial y}, \tag{3}$$

along with the corresponding boundary conditions:

- at $y = 0$:

$$u=U_w(x)=ae^{\frac{x}{L}}, v=0,\quad T=T_w=T_\infty+T_0e^{\frac{x}{2L}}, \tag{4}$$

- as $y\to\infty$:

$$u\longrightarrow 0,\qquad T\longrightarrow T_\infty, \tag{5}$$

where (u,v) denote the velocity components of the nanofluid in the x- and y-directions, respectively, $U_w(x)$ is the velocity of the exponentially stretching sheet, K denotes the porous medium permeability, T is the nanofluid temperature, T_∞ represents the free stream temperature, T_w is the temperature of the sheet surface of the hot fluid below the sheet, ρ_{nf} represents the nanofluid density, μ_{nf} is the nanofluid dynamic viscosity, k_{nf} denotes the nanofluid thermal conductivity, $(\rho C_p)_{nf}$ is the nanofluid heat capacitance, L is characteristic length and σ_{nf} is the nanofluid electrical conductivity. It is important to note from the boundary conditions in Eq. (4) that the surface of the exponentially stretching sheet is impermeable and maintained at a non-uniform temperature that increases along the sheet. Following [32], the thermophysical expressions relating ferrofluids to base fluid and nanoparticles are given as follows:

$$\rho_{nf}=(1-\phi)\rho_f+\phi\rho_s,\qquad \mu_{nf}=\frac{\mu_f}{(1-\phi)^{2.5}}, \tag{6a}$$

$$(\rho C_p)_{nf}=(1-\phi)(\rho C_p)_f+\phi(\rho C_p)_s,\qquad r=\frac{\sigma_s}{\sigma_f}, \tag{6b}$$

$$\frac{k_{nf}}{k_f}=\frac{k_s+2k_f-2\phi(k_f-k_s)}{k_s+2k_f+\phi(k_f-k_s)},\qquad \frac{\sigma_{nf}}{\sigma_f}=1+\frac{3(r-1)\phi}{(r+2)-(r-1)\phi}, \tag{6c}$$

where ρ_f refers to the density of the base fluid, ρ_s is the density of the solid nanoparticle, k_f is the base fluid thermal conductivity, k_s is the thermal conductivity of the nanoparticles, σ_f is the electrical conductivity of the base fluid, σ_s is the electrical conductivity of the nanoparticles, ϕ represents the volume fraction of the nanoparticles, μ_f is the base fluid's dynamic viscosity C_{pf} is the specific heat capacity of the base fluid, and C_{ps} is the specific heat capacity of the nanoparticles. The physical properties of H_2O and Fe_3O_4 nanoparticles are listed in Table 1 below.

Table 1. Nanoparticles and base fluid thermophysical properties [33].

Physical properties	ρ, kg/m³	C_p, J/(kg·K)	k, W/(m·K)	σ, S/m
H_2O	997.1	4179	0.613	5×10^{-5}
Fe_3O_4	5180	670	9.7	2.5×10^{6}

Based on the Roseland approximation [34], the local radiative heat flux term for optically thick gray nanofluid can be written as:

$$q_r=-\frac{4\sigma^*}{3k^*}\frac{\partial T^4}{\partial y}\approx-\frac{16\sigma^*T_\infty^3}{3k^*}\frac{\partial T}{\partial y}, \tag{7}$$

where $T^4 \approx 4T_\infty{}^3T - 3T_\infty{}^4$ (by employing the Taylor series approximation), k^* denotes the mean absorption coefficient, and σ^* is the Stefan-Boltzmann constant.

Thus,

$$\frac{\partial q_r}{\partial y} \approx -\frac{16\sigma^* T_\infty^3}{3k^*}\frac{\partial^2 T}{\partial y^2}. \quad (8)$$

Inserting Eq. (8) into Eq. (3), we obtain the energy balance equation as:

$$\frac{(\rho c_p)_{nf}}{k_f}\left(u\frac{\partial T}{\partial x}+v\frac{\partial T}{\partial y}\right)=\left[\left(\frac{k_{nf}}{k_f}\right)+\frac{16\sigma^* T_\infty^3}{3k^* k_f}\right]\frac{\partial^2 T}{\partial y^2}+ +\frac{\mu_{nf}}{k_f}\left(\frac{\partial u}{\partial y}\right)^2+\left(\frac{\mu_{nf}}{k_f K}+\frac{\sigma_{nf}B_0^2}{k_f}\right)u^2 \quad (9)$$

Similarity transformations defined below are considered to simplify the governing partial differential equations into a system of ordinary differential equations

$$\eta = ye^{\frac{x}{2L}}\sqrt{\frac{a}{2\nu_f L}}, \qquad v=-e^{\frac{x}{2L}}\sqrt{\frac{a\nu_f}{2L}}\left(\eta f'(\eta)+f(\eta)\right),$$

$$M=\frac{\sigma_f B_0^2 L}{\rho_f U_w}, \quad A_5=\frac{(\rho C_p)_{nf}}{(\rho C_p)_f}, \quad A_1=\frac{\mu_{nf}}{\mu_f}, \quad A_2=\frac{\rho_{nf}}{\rho_f},$$

$$A_3=\frac{k_{nf}}{k_f}, \quad \mathrm{Ec}=\frac{U_w^2}{C_{pf}(T_w-T_\infty)}, \quad u=ae^{\frac{x}{L}}f'(\eta),$$

$$A_4=\frac{\sigma_{nf}}{\sigma_f}, \qquad \theta=\frac{T-T_\infty}{T_w-T_\infty}, \qquad T_w=T_\infty+T_0e^{\frac{x}{2L}},$$

$$\mathrm{Da}=\frac{KU_w}{\nu_f L}, \qquad \mathrm{Ra}=\frac{4\sigma^* T_\infty^3}{k^* k_f}, \qquad \mathrm{Pr}=\frac{\mu_f C_{pf}}{k_f}. \quad (10)$$

Substituting Eq. (10) into Eqs. (2)–(9), we obtain the following local similarity equations:

$$f'''+\frac{A_2}{A_1}[ff''-2(f')^2]-2\left(\frac{A_4}{A_1}M+\frac{1}{\mathrm{Da}}\right)f'=0, \quad (11)$$

$$\left(A_3+\frac{4Ra}{3}\right)\theta''+A_5\mathrm{Pr}[f\theta'-f'\theta]+A_1\mathrm{PrEc}(f'')^2+ +\mathrm{PrEc}\left(A_4M+\frac{A_1}{\mathrm{Da}}\right)(f')^2=0 \quad (12)$$

with the associated boundary conditions given as:

- at $y = 0$:

$$f'(\eta)=1, \qquad f(\eta)=0, \qquad \theta(\eta)=1 \quad (13a)$$

- as $y \to \infty$:

$$f'(\eta)=0, \qquad \theta(\eta)=0, \quad (13b)$$

where Pr (≈6.2) is the Prandtl number (for water-based nanofluid), *Ra* is the thermal radiation parameter, with *M* as the magnetic field parameter, Ec is the Eckert number, and Da is the Darcy number. Other related quantities of interest include the skin friction coefficients (C_f) and the Nusselt number (Nu), which are given as:

$$C_f\,\mathrm{Re}_x^{1/2}=A_1\frac{d^2f}{d\eta^2}(0), \quad (14a)$$

$$\mathrm{Nu}\,\mathrm{Re}_x^{-1/2}=-\left(A_3+\frac{4\mathrm{Ra}}{3}\right)\frac{d\theta}{d\eta}(0), \quad (14b)$$

where:

$$C_f=\frac{\tau_w}{\rho_f U_w^2}, \qquad \mathrm{Nu}=\frac{xq_w}{k_f(T_f-T_\infty)}, \qquad \tau_w=\mu_{nf}\frac{\partial u}{\partial y}, \quad (15a)$$

$$q_w=-\left(k_{nf}+\frac{16\sigma^* T_\infty^3}{3k^*}\right)\frac{\partial T}{\partial y}, \qquad \mathrm{Re}_x=\frac{xU_w}{\upsilon_f}. \quad (15b)$$

3. Numerical procedure

The nonlinear boundary value problem defined by Eqs. (11) and (12), along with the boundary conditions specified in Eq. (13), is solved numerically using the shooting method combined with the Runge-Kutta-Fehlberg integration technique [30–31]. To facilitate this approach, the boundary value problem (BVP) is reformulated as an initial value problem (IVP), and numerical integration is carried out using the Runge-Kutta-Fehlberg method (RKF45). To implement the method, new variables are introduced to represent the derivatives, such that:

$$f_1=f, f_2=f', f_3=f'', \theta_1=\theta, \theta_2=\theta'. \quad (16)$$

Implementing Eq. (16), transform Eqs. (11)–(13) to:

$$f_3'=\frac{A_2}{A_1}(2f_2^2-f_3f_1)+2f_2\left(\frac{A_4}{A_1}M+\frac{1}{\mathrm{Da}}\right), \quad (17)$$

$$\theta_2'=\frac{A_5\mathrm{Pr}(f_2\theta_1-f_1\theta_2)-A_1\mathrm{PrEc}f_3^2-\mathrm{PrEc}f_2^2\left(A_4M+\frac{A_1}{\mathrm{Da}}\right)}{A_3+\frac{4Ra}{3}}, \quad (18)$$

with initial conditions:

$$f_2(0)=1, \qquad f_1(0)=0, \qquad \theta_1(0)=1,$$
$$f_3(0)=a_1, \qquad \theta_2(0)=a_2. \quad (19)$$

The unspecified, initial values of a_1 and a_2 that emerged in Eq. (19) are first assumed, and then the values are estimated accurately through a shooting methodology using an iterative method employing Newton-Raphson's method. We define the first-order system of ODEs for *f* and θ as:

$$\boldsymbol{y}'=\boldsymbol{F}(\eta,y), \quad (20)$$

where $\boldsymbol{y} = [f_1, f_2, f_3, \theta_1, \theta_2]^T$ and the components of $\boldsymbol{F}(\eta, y)$ are derivatives of Eqs. (16)–(18), and thereafter, the Runge-Kutta-Fehlberg integration scheme is applied. To validate the accuracy of our numerical procedure and benchmark the present results, we compare a special case from this study with previously published values of the skin friction coefficient reported in Refs. [36,37] for the conditions $\phi = 0$ and $\mathrm{Da} \to \infty$, as presented in Table 2. The comparison demonstrates excellent agreement both qualitatively and quantitatively.

Table 2. Comparative data of $f''(0)$ for $2M$ when $\phi = 0$, $\mathrm{Da} \to \infty$.

2M	Ref. [36]	Ref. [37]	Present
0.0	1.0000	1.0000	1.00000
0.25	1.1180	1.1180	1.11803
1.0	1.4137	1.4142	1.41421
5.0	2.4495	2.4495	2.44949
10	3.3166	3.3166	3.31662

2. Results and discussion

The graphical results derived from Eqs. (11) to (13) vividly illustrate the influence of key thermophysical flow parameters on the behaviour of nanofluid motion within porous and magnetically influenced environments, with direct relevance to various industrial and engineering systems. Figure 2 emphasises the role of the porous medium's permeability, quantified by the Darcy numer, in the velocity distribution. As the Darcy number increases, indicating a more permeable medium, the fluid experiences reduced resistance due to lower drag forces imposed by the solid matrix. This results in a broadened momentum boundary layer and enhanced nanofluid velocity, which is critical for optimising flow systems such as packed-bed reactors, geothermal reservoirs, and filtration devices, where controlled permeability is essential for performance.

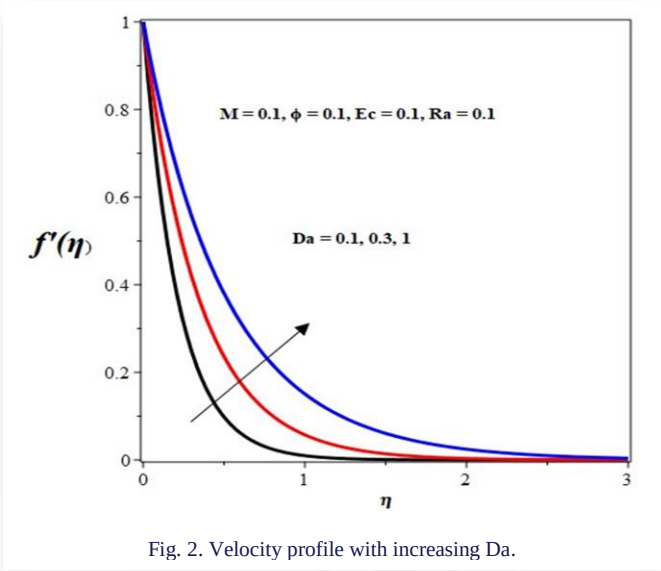

Fig. 2. Velocity profile with increasing Da.

Figure 3 shows how the strength of the magnetic field affects the fluid's speed, demonstrating that the Lorentz force works against the fluid's movement, which slows it down. At a nanoparticle concentration of 10%, the magnetic field's damping effect becomes more pronounced, especially in regions away from the boundary, eventually causing the velocity to approach zero in the free stream. Strong magnetic fields effectively draw the nanofluid closer to the heated surface, compressing the momentum boundary layer and thereby enhancing surface heat absorption.

This MHD behaviour is particularly advantageous in applications such as electromagnetic pumps, nuclear reactor cooling systems, and advanced cooling technologies in electronics and metallurgy, where precise control over flow and heat transfer is vital. Additionally, being able to control fluid flow and transfer heat by adjusting permeability and magnetic fields allows for the creation of advanced thermal systems and nanofluid heat exchangers in fields like aerospace, healthcare, and energy conversion.

Figures 4 to 8 clearly show how important thermophysical factors affect temperature distribution in the flow problem being studied, which is important for various engineering and industrial uses like thermal management systems, energy devices, and material processing. Figure 4 shows that when the porous material allows more fluid to pass through, it improves heat transfer by convection rather than conduction because there is less resistance to the fluid's movement. In areas with low porosity, high friction creates a lot of internal heat, but as porosity increases, this heat is reduced, leading to lower temperatures. This is especially important in fields like geothermal engineering, filtration systems, and catalytic reactors where porous materials are essential.

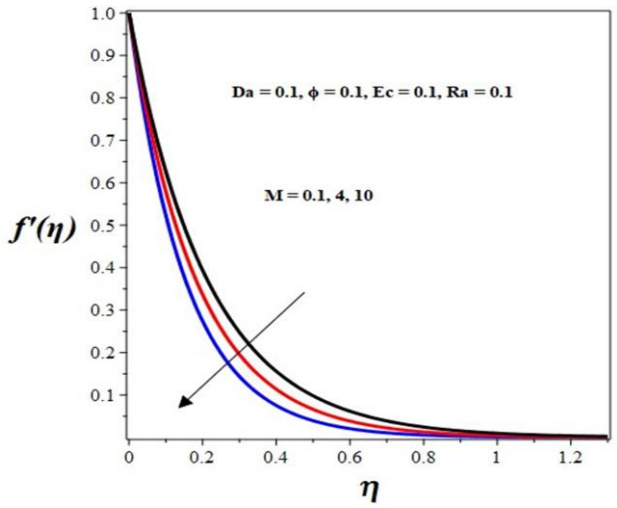

Fig. 3. Velocity profile with increasing *M*.

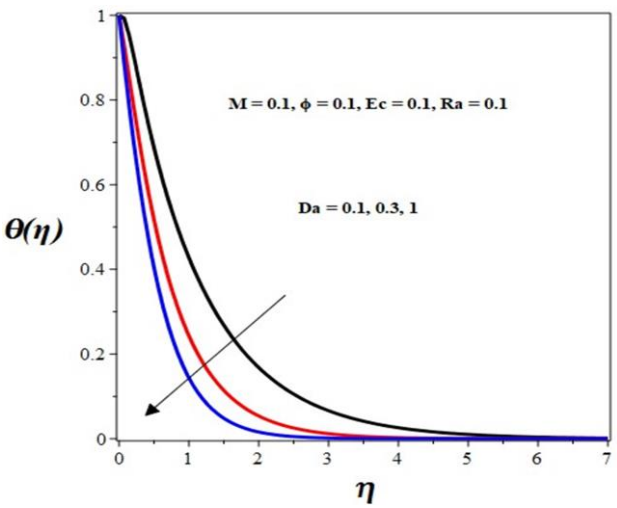

Fig. 4. Temperature profile with increasing Da.

Figure 5 shows that the introduction of the magnetic field imposes a Lorentz force that resists fluid flow and induces Joule heating by transforming kinetic energy into thermal energy. This results in a higher temperature within the boundary layer, especially near the surface, making magnetic control valuable in MHD power generators, plasma confinement, and metallurgical cooling processes. Figure 6 emphasises the role of thermal radiation, where increased radiative heat transfer augments the effective thermal conductivity of nanofluids. This mechanism, vital in high-temperature environments such as aerospace thermal shields and solar energy collectors, promotes enhanced thermal

dispersion and results in elevated fluid temperatures. In Fig. 7, the impact of the Eckert number, representing viscous dissipation, becomes apparent: as this parameter rises, the conversion of kinetic energy into thermal energy intensifies, particularly near the heated plate surface, where velocity gradients are steep. This phenomenon is critical in high-speed fluid applications like turbine blade cooling and polymer extrusion processes.

Finally, Fig. 8 underscores the importance of nanoparticle volume fraction in nanofluid behaviour. An increase from 5% to 10% significantly thickens the thermal boundary layer and accelerates heat transfer, leading to a marked temperature rise. Such behaviour is highly advantageous in advanced heat exchangers, electronic cooling systems, and biomedical applications, where precise thermal control and efficient heat dispersal are paramount. Collectively, these findings underscore the pivotal role of thermophysical parameter tuning in optimising thermal performance across a wide range of engineering domains.

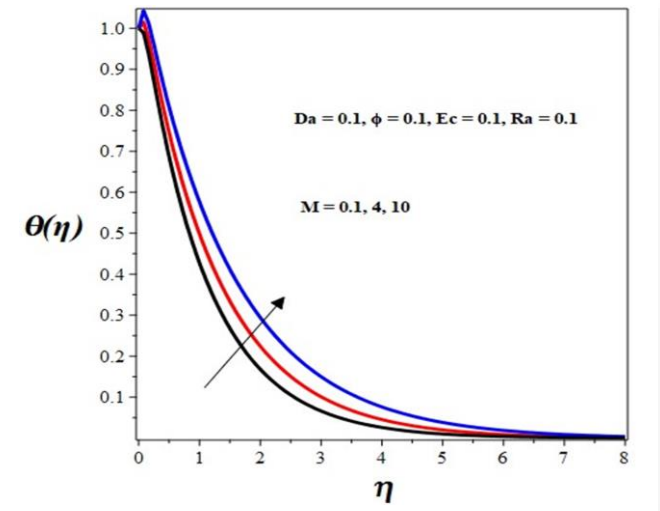

Fig. 5. Temperature profile with increasing *M*.

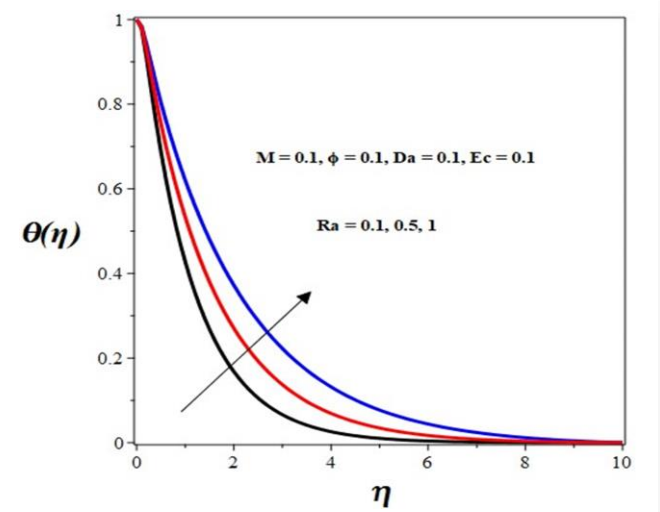

Fig. 6. Temperature profile with increasing Ra.

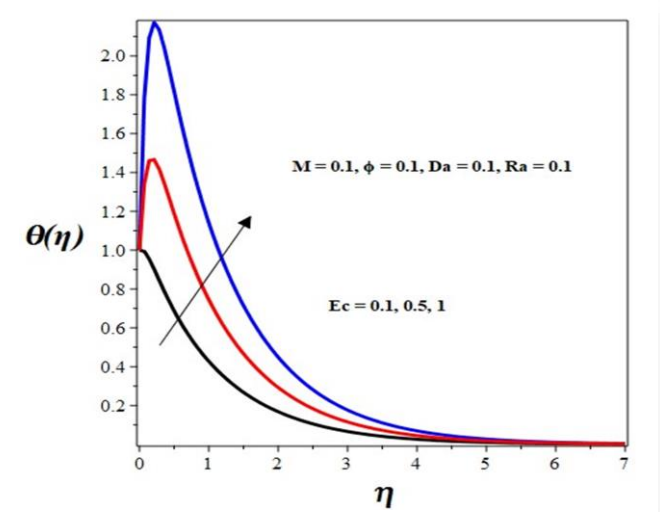

Fig. 7. Temperature profile with increasing Ec.

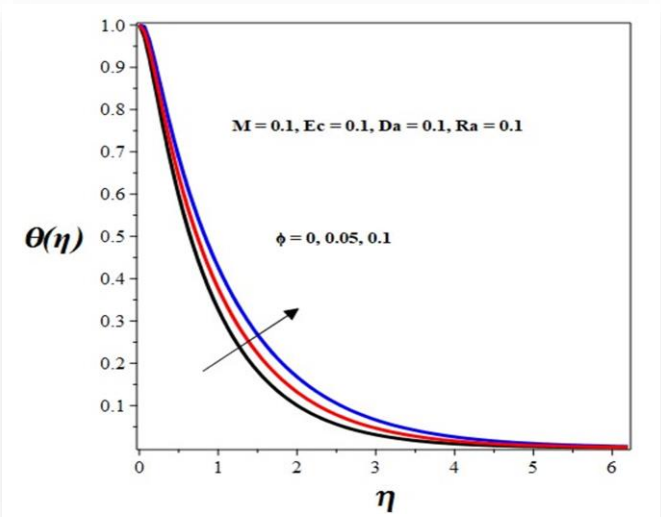

Fig. 8. Temperature profile with increasing ϕ.

Figures 9 to 11 show how the magnetic field parameter, Darcy number, nanoparticle volume fraction, and thermal radiation interact and affect the skin friction and Nusselt number, which are important in fluid dynamics and heat transfer. Figure 9 shows that when the magnetic field parameter is increased, skin friction goes up because the Lorentz force makes it harder for the fluid to move, pushing the flow closer to the surface and increasing resistance and possible wear on the surface. This effect is especially important in MHD applications like cooling nuclear reactors, using electromagnetic pumps, and in metal processing, where controlling fluid movement is essential. The amount of nanoparticles in a fluid is important; when there are more nanoparticles, it increases skin friction because the fluid becomes denser and thicker. This is especially important in areas like targeted drug delivery, solar energy systems, and managing heat in electronics. The Darcy number, which shows how easily fluid can flow through a porous material, is very important; low Darcy values mean less space for fluid to move, causing more friction, while higher values allow fluid to flow more easily and reduce friction, which is essential for creating efficient packed bed reactors, geothermal reservoirs, and filtration systems. Figure 10 shows that having too many particles in the mixture lowers the Nusselt number, meaning that too many

nanoparticles can act as an insulator and reduce heat flow. This information is important for optimising heat exchangers and thermal interface materials. Moreover, as the Darcy number increases, heat transfer at the surface improves due to enhanced convective flow, while stronger magnetic fields suppress the Nusselt number by impeding thermal boundary layer motion – key in applications involving MHD flows in aerospace engineering and advanced energy systems.

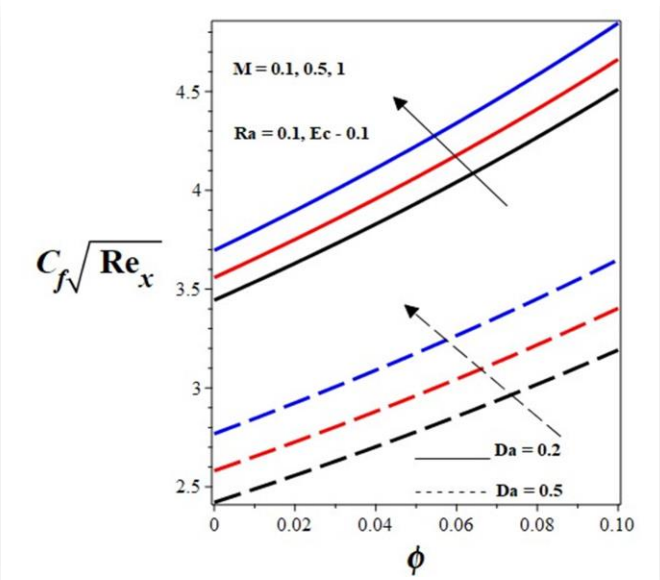

Fig. 9. Skin friction with increasing *M* and Da versus ϕ.

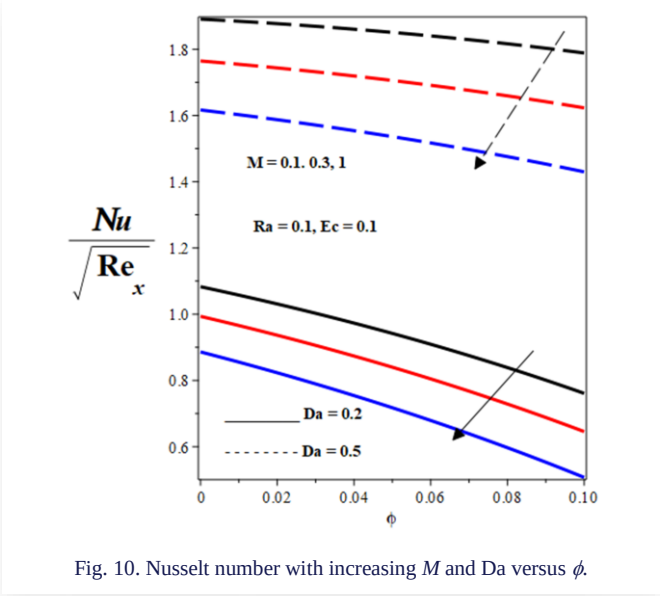

Fig. 10. Nusselt number with increasing *M* and Da versus ϕ.

Finally, Fig. 11 shows that both magnetic fields and thermal radiation significantly lower the Nusselt number, which means they reduce the ability to transfer heat through convection. This phenomenon has significant implications in high-temperature environments such as space vehicle thermal shields, radiative cooling systems, and solar thermal power plants, where understanding and mitigating heat transfer suppression due to electromagnetic and radiative forces is essential for maintaining performance and structural integrity.

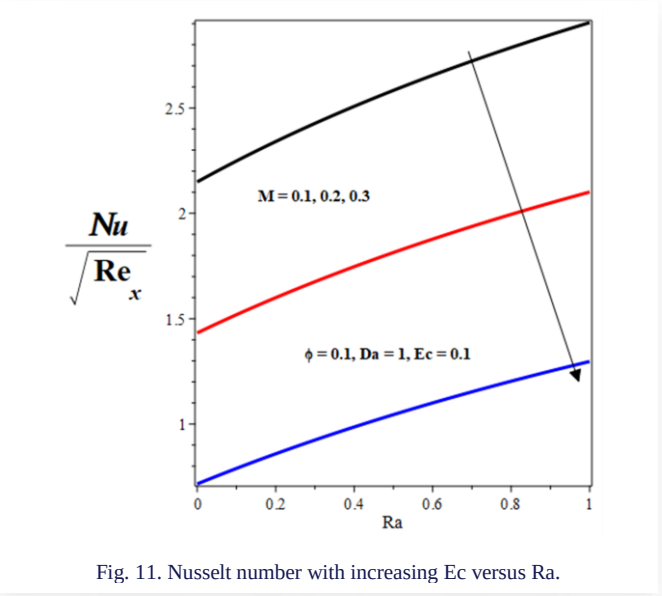

Fig. 11. Nusselt number with increasing Ec versus Ra.

5. Conclusions

This study examines the hydromagnetic convective flow of a radiating nanofluid past an exponentially stretching sheet embedded in a porous medium. The shooting numerical technique coupled with the Runge-Kutta-Fehlberg integration scheme is employed to tackle the nonlinear model problem. We present graphically and discuss pertinent results on the effects of various thermophysical parameters on the overall flow structure and thermal enhancement. The research elaborates its findings as follows:

- The Darcy number, which measures the permeability of the porous medium, increases fluid velocity by reducing flow resistance, impacting fields like filtration, petroleum engineering, and soil mechanics. In contrast, a magnetic field slows down fluid velocity due to the MHD effect, where the magnetic field interacts with charged particles in the fluid. This effect is important in industries like nuclear reactors, electrical power generation, and materials processing, where magnetic fields are used to control or stabilise fluid flows, especially in high-temperature environments.
- The study shows that the magnetic field and thermal radiation parameters increase the fluid's temperature profile, while the Eckert number raises the temperature by converting kinetic energy to thermal energy. Increased nanoparticle volume enhances thermal conductivity, boosting the temperature profile, while a higher Darcy number reduces the temperature by lowering the fluid's residence time in porous media. These factors are crucial in applications like cooling systems, aerospace, high-speed fluid flow, heat exchangers, and geothermal energy systems.
- The skin friction increases with a growing magnetic field, higher Darcy numbers, and larger nanoparticle volume fractions. The MHD effect raises viscous drag, while

higher Darcy numbers and nanoparticle concentrations enhance fluid viscosity, leading to more friction. These factors are critical in designing efficient fluid flow systems, porous media-based filtration, and catalysis, where minimising frictional losses is essential.

- The Nusselt number, representing convective heat transfer, decreases with higher magnetic field strength, as does the Darcy number, reducing heat transfer efficiency in systems like heat exchangers and reactors. A higher amount of nanoparticles makes it harder for heat to transfer in cooling systems because it thickens the layer of heat around them. Also, when stronger magnetic fields and more thermal radiation work together, they further lower the Nusselt number, showing the balance between radiation and convection, which is crucial in high-temperature industries like materials processing and aerospace.

The study's findings are relevant to several industrial applications involving fluid flow in porous media, heat transfer, and nanofluids. These include energy systems (geothermal, oil recovery, and heat exchangers), where managing Darcy numbers, magnetic fields, and nanoparticle contents enhances efficiency. Nanofluids are also used in cooling systems for electronics, automotive engines, and industrial heat exchangers, where controlling nanoparticle volume and magnetic fields optimises performance. In chemical engineering, these results benefit processes like catalysis and filtration by improving fluid flow and heat transfer. Additionally, the findings assist in managing heat dissipation in aerospace and high-temperature systems like combustion chambers and nuclear reactors. Overall, the study provides valuable insights for optimising heat transfer and flow in various engineering applications. In the future, this study will be broadened to look into how changes in flow, shrinking and slippery surfaces, the effects of porous materials, entropy, thermophoresis, and the movement of nanoparticles affect the results.

References

[1] Abbas, N., Shatanawi, W., Hasan, F., & Shatnawi Taqi, A.M. (2025). Investigation of MHD radiative Casson micropolar hybrid nanofluid over an exponential curved stretching sheet. *Journal of Radiation Research and Applied Sciences*, 18(1), 101269. doi: 10.1016/j.jrras.2024.101269

[2] Nayak, M.K., Pandey, V.S., Tripathi, D., Akbar, N.S., & Makinde, O.D. (2020). 3D MHD cross flow over an exponential stretching porous surface. *Heat Transfer*, 49(3), 1256−1280. doi: 10.1002/htj.21661

[3] Crane, L.J. (1970). Flow past a stretching plate. *Journal of Applied Mathematics and Physics ournal of Applied Mathematics and Physics* (*Zeitschrift für Angewandte Mathematik und Physik*), 21, 645−647. doi: 10.1007/BF01587695

[4] Elbashbeshy, E.M.A. (1998). Heat transfer over a stretching surface with variable surface heat flux. *Journal of Physics. D: Applied Physics*, 31(16), 1951−1954.

[5] Mahapatra, T.R., & Gupta, A.S. (2002). Heat transfer in stagnation-point flow towards a stretching sheet. *Heat and Mass Transfer*, 38, 517−521. doi: 10.1007/s002310100215

[6] Chaudhary, S., Choudhary, M.K., & Sharma, R. (2015). Effects of thermal radiation on hydromagnetic flow over an unsteady stretching sheet embedded in a porous medium in the presence of a heat source or sink. *Meccanica*, 50, 1977–1987. doi: 10.1007/s11012-015-0137-9

[7] Alkaoud, A., Khader, M.M., Eid., A. & Megahed, A.M. (2024). Numerical simulation of the flow of a tangent hyperbolic fluid over a stretching sheet within a porous medium, accounting for slip conditions. *Heliyon*, 10, e28683. doi: 10.1016/j.heliyon.2024.e28683

[8] Nawaz, Y., Arif, M.S., Nazeer, A., Abbasi, J.N., & Abodayeh, K. (2024). A two-stage reliable computational scheme for stochastic unsteady mixed convection flow of Casson nanofluid. *International Journal for Numerical Methods in Fluids*, 96(5), 719–737. doi: 10.1002/fld.5264

[9] Saleem, M., Hussain, M., & Inc, M. (2023). Significance of Darcy–Forchheimer law and magnetic field on the comparison of Williamson–Casson fluid subject to an exponential stretching sheet. *International Journal of Modern Physics B*, 37(27), 2350315. doi: 10.1142/S0217979223503150

[10] Vajravelu, K., & Roper, T. (1999). Flow and heat transfer in a second-grade fluid over a stretching sheet. *International Journal of Non-linear Mechanics*, 34(6), 1031–1036. doi: 10.1016/S0020-7462(98)00073-0

[11] Sajid, M., Ali, N., Javed, T., & Abbas, Z. (2010). Stretching a curved surface in a viscous fluid. *Chinese Physics Letters*, 27(2), 024703. doi: 10.1088/0256-307X/27/2/024703

[12] Abbas, Z., Naveed, M., & Sajid, M. (2016). Hydromagnetic slip flow of nanofluid over a curved stretching surface with heat generation and thermal radiation. *Journal of Molecular Liquids*, 215, 756–762. doi: 10.1016/j.molliq.2016.01.012

[13] Hussain, Z., Hayat, T., Alsaedi, A., & Anwar, M.S. (2021). Mixed convective flow of CNTs nanofluid subject to varying viscosity and reactions. *Scientific Reports*, 11, 22838. doi: 10.1038/s41598-021-02228-9

[14] Othman, M.N., Jedi, A., & Bakar, N.A.A. (2021). MHD stagnation point on nanofluid flow and heat transfer of carbon nanotube over a shrinking surface with heat sink effect. *Molecules*, 26, 7441. doi: 10.3390/molecules26247441

[15] Majeed, A., Zeeshan, A., & Alam, T. (2023). Mathematical analysis of MHD CNTs of rotating nanofluid flow over a permeable stretching surface. *Arab J. Sci. Eng*, 48, 727–737, doi: 10.1007/s13369-022-06871-w

[16] Choudhary, P., Choudhary, S., Jat, K., Loganathan., K., & Eswaramoorthi, S. (2024). Impacts of unsteady MHD hybrid nanofluid over a non-linear stretchable porous sheet with thermal radiation and gyrotactic microorganisms. *International Journal of Thermofluids*, 23, 100788, doi: 10.1016/j.ijft.2024.100788

[17] Sharma, R.P., Baag, S., Mishra, S.R., & Sahoo, P. (2023). On the radiative heat transport phenomena in MHD Williamson nanofluid flow past an expanding surface with an interaction of inclined magnetic field. *Journal of Thermal Analysis Calorimetry*, 148(14). doi: 10.1007/s10973-023-12206-0

[18] Sakkaravarthi, K., & Reddy, B.A. (2023). Entropy generation on MHD Casson and Williamson hybrid nanofluid over a curved stretching sheet with the Cattaneo–Christov heat flux model: semi-analytical and numerical simulations. *International Journal of Ambient Energy*, 44(1). doi: 10.1080/01430750.2023. 2190338

[19] Makinde, O.D., & Eegunjobi, A.S. (2017). MHD couple stress nanofluid flow in a permeable wall channel with entropy generation and nonlinear radiative heat. *Journal of Thermal Science and Technology*, 12(2). doi: 10.1299/jtst.2017jtst0033

[20] Srinivasulu, T., & Goud, B.S.(2021). Effect of inclined magnetic field on flow, heat, and mass transfer of Williamson nanofluid over a stretching sheet, *Case Stuies in. Thermal Engineering*, 23, 100819. doi: 10.1016/j.csite.2020.100819

[21] Kiwan, S., & Ali, M.E .(2008). Near-slit effects on the flow and heat transfer from a stretching plate in a porous medium. *Numerical Heat Transfer, Part A: Applications*, 54(1), 93–108. doi: 10.1080/10407780802025275

[22] Tamayol, A., Hooman, K., & Bahrami, M. (2010). Thermal analysis of flow in a porous medium over a permeable stretching wall. *Transport in Porous Media*, 85(3), 661–676. doi: 10.1007/s11242-010-9584-x

[23] Pal, D., & Chatterjee, S. (2010). Heat and mass transfer in MHD non-Darcian flow of a micropolar fluid over a stretching sheet embedded in a porous medium with non-uniform heat source and thermal radiation. *Communications in Nonlinear Science and Numerical Simulation*, 15(7), 1843–1857. doi: 10.1016/j.cnsns.2009.07.024

[24] Krishna, M.V., Ahammad, N.A., & Chamkha, A.J. (2021). Radiative MHD flow of Casson hybrid nanofluid over an infinite exponentially accelerated vertical porous surface. *Case Studies in Thermal Engineering*, 27, 101229. doi: 10.1016/j.csite.2021.101229

[25] Eegunjobi, A.S., & Makinde, O.D. (2014). Second law analysis for MHD permeable channel flow with variable electrical conductivity and asymmetric Navier slips. *Open Physics*, 13(1), 100−110, doi: 10.1515/phys-2015-0014.

[26] Chamkha, A. J, Issa, C., & Khanafer, K. (2002). Natural convection from an inclined plate embedded in a variable porosity porous medium due to solar radiation. *Intenatinal Journal of Thermal Sciences*, 41(1), 73–81. doi: 10.1016/S1290-0729(01)01305-9

[27] Makinde, O.D., & Sibanda, P. (2008). Magnetohydrodynamic mixed convective flow and heat and mass transfer past a vertical plate in a porous medium with constant wall suction. *Journal of Heat Transfer*, 130(11). doi: 10.1115/1.2955471

[28] Hayat, T., Qasim, M., & Mesloub, S. (2011). MHD flow and heat transfer over permeable stretching sheet with slip conditions. *International Journal for Numerical Methods in Fluids*, 66, 963−675. doi: 10.1002/fld.2294

[29] Khan, M.S., Karim, I., Islam, M.S., & Wahiduzzaman, M. (2014). MHD boundary layer radiative, heat-generating, and chemical reacting flow past a wedge moving in a nanofluid. *Nano Convergence*, 1(20). doi: 10.1186/s40580-014-0020-8

[30] Cebeci, T., & Bradshaw, P. (1988). *Physical and computational aspects of convective heat transfer*. New York, USA, Springer.

[31] Na, T.Y. (1979). *Computational methods in engineering boundary value problems*. Academic Press. New York.

[32] Brinkman, H.C. (1952). The viscosity of concentrated suspensions and solutions. *The Journal of Chemical Physics*, 20(4), 571−571. doi: 10.1063/1.1700493

[33] Kefene, Z.M., Makinde, O.D., & Enyadene, G.L. (2022). Magnetic Effects of Ferrofluid Flow in a Heated Micro-Channel with Permeable Walls. *Latin American Applied Research*, 52(3), 247−257. doi: 10.52292/j.laar.2022.666

[34] Eegunjobi, A.S., & Makinde, O.D. (2017). Irreversibility analysis of hydromagnetic flow of couple stress fluid with radiative heat in a channel filled with a porous medium. *Results in Physics*, 7, 459−469. doi: 10.1016/j.rinp.2017.01.002

[35] Putra, N., Roetzel, W. & Das, S.K., (2003). Natural convection of nanofluids. *Heat and Mass Transfer*, 39, 775–784. doi: 10.1007/s00231-002-0382-z

[36] Waqas, H., Kafait, A., Muhammad, T., & Farooq, U. (2022). Numerical study for bio-convection flow of tangent hyperbolic nanofluid over a Riga plate with activation energy. *Alexandria Engineering Journal.*, 61(2), 1803−1814. doi: 10.1016/j.aej.2021.06.068

[37] Amjad, M., Khan, M.N., Ahmed, K., Ahmed, I., Akbar, T., & Eldin, S.M., (2023). Magnetohydrodynamics tangent hyperbolic nanofluid flow over an exponentially stretching sheet: Numerical investigation. *Case Studies in Thermal Engineering*, 45, 102900. doi: 10.1016/j.csite.2023.102900

[38] Chamkha, A.J., & Pop, I. (2004). Effect of thermophoresis particle deposition in free convection boundary layer from a vertical flat plate embedded in a porous medium. *International Communications in Heat and Mass Transfer*, 31(3), 421−430. doi: 10.1016/j.icheatmasstransfer.2004.02.012